



**8th International Conference
on
Wind Turbine Noise
Lisbon – 12th to 14th June 2019**

A Wind Turbine Noise Code Benchmark - Round 1

Franck Bertagnolio
DTU Wind Energy, Roskilde, DK-4000, Denmark

Second C. Author
Institution, City, Province, Zip Code, Country

Summary

The aim of this study is to compare and validate wind turbine noise prediction codes from various institutes and companies. This effort is part of the IEA Wind TCP Task 29 (Wind Turbine Aerodynamics) and IEA Wind TCP Task 39 (Quiet Wind Turbine Technology). The benchmark is divided into 3 rounds which will be dealt with incrementally in time, and the focus of the present article is on the first round. Note that this study concentrates on aerodynamic noise generation, therefore mechanical noise and long-range atmospheric propagation effects are not considered.

1. Introduction

Wind turbine noise emissions are commonly measured in the field according to the IEC-64100-11 standard [4]. Microphones are placed on the ground downstream of the turbine at a specified distance from the tower (equal to the height of the tower plus half of the rotor diameter). The wind turbine is considered as a monopole noise source and is thereby supposed to emit the same noise levels in all directions. Thus, the measured sound pressure levels can be related to the sound power levels of the turbine. Immission levels at dwellings can be evaluated using a variety of methods predicting the propagation losses, from simple semi-empirical formulas to advanced simulation methods such as Parabolic Equations or Computational Aero-Acoustics. Furthermore, the results of the above standardized measurements are binned according to the wind speed to reflect the actual variations of the noise emission levels with respect to the wind conditions. Modern turbines produce typically less

noise at low wind speed because of the lower rotational speed, and nearly constant noise above rated power when the rotational speed is normally kept fixed and power is regulated by the controller through the blade pitch.

However, as far as the actual noise emissions are concerned (i.e. when considering the wind turbine as the source of noise), the physics of noise generation mechanisms is more complicated than the above conceptualization. The assumption of a monopole noise source is certainly a first order approximation. Nevertheless, note that for wind turbine certification it is considered as satisfying to measure according to the IEC-64100-11 standard since microphones should be located directly downstream of the turbine, where the maximum noise levels are expected. In this sense, the IEC standard is a worst case situation. Yet, the noise generation mechanisms (e.g. trailing edge noise considered as one of the most potent source of noise in the audible range) present strong directivity features [1, 3]. These effects are not accounted for in the measurements according to the above standard.

Another aspect of wind turbine noise is the fact that multiple noise generation mechanisms are simultaneously at play. These can be segregated in two main categories: mechanical and aerodynamic noise. Mechanical noise results from structural vibrations of the turbine components (tower, nacelle and blades) as well as gear noise. Usually, it is identified as tonal noise with frequencies associated to the eigenfrequencies of these components or to the rotational speed of the shaft or the gear components. Although potentially annoying and subject to regulations related to tonal noise, mechanical noise is not considered herein. The present study concentrates on aerodynamic noise, i.e. noise generated by the interaction of turbulent vortices with the blade surfaces. These turbulent features can be self-generated, as it is the case for the turbulent boundary layer flow developing along the blade airfoil sections producing noise when passing by the trailing edge. Alternatively, they can originate from the turbulent atmospheric flow impacting the blades or some other external source of turbulence (e.g. wake from an upstream turbine).

Aerodynamic noise generation involves complex phenomena and their mutual interactions. Firstly, fluid flow turbulence is a difficult topic with highly non-linear processes which are not trivial to predict. Most of the theory of turbulence is based on statistical averaging which somehow facilitates some aspects of flow prediction in contrast to the deterministic prediction of the chaotic behavior of the turbulent structures. This is quite relevant for wind turbine noise generation since the time-scales of the turbulent motions generating noise are quite small compared to the time-scales of the parameters influencing the wind turbine operation (e.g. changing mean wind speed over the rotor disk or rotational speed). Secondly, turbulence interaction with the hard surfaces generating noise are also rather complicated phenomena, e.g. noise scattering at the trailing edge. As a consequence, accurately predicting noise from wind turbines can be challenging.

Wind turbine manufacturers have a long practical experience of noise emissions from their wind turbines and have access to a lot of noise measurement data. To predict the noise emission from a turbine, in many cases they rely on semi-empirical models which can be accurately tuned thanks to the above practical experience and know-how. The next step in developing modeling tools capable of predicting wind turbine noise is to introduce more physics in the models and try to describe more faithfully the actual processes involved. This may become a critical asset as wind turbine technology develops with the use of advanced aerodynamic features such as flaps, morphing blades, winglets, etc.

To the best authors' knowledge, there does not exist a commercial simulation tool that is dedicated to the prediction of wind turbine noise as a source, although several of these codes can be used in this context []. As a result, wind turbine manufacturers and research institutions alike separately are developing their own prediction tools. When wind turbine manufacturers can rely on their expertise and historical data, it is sometimes difficult for the researchers to find reliable data to validate their models. Contrastingly, the manufacturers do sometimes have limited resources to develop more advanced simulation tools and usually rely on their existing more empirical tools. In both cases, exchanging experience and comparing results may benefit the two communities.

The aim of the present study is to define a comparison benchmark for wind turbine noise simulation codes. This initiative was taken as part of IEA Wind TCP Task 39 (Quiet Wind Turbine Technology) in collaboration with IEA Wind TCP Task 29 (Analysis of Aerodynamic Measurements). The comparisons are based on an existing wind turbine which was extensively measured during the DANAERO project [5, 6]. These measurements were conducted on a 2.3 MW NM80 wind turbine located in Tjæreborg, Denmark. One of the blades was specifically manufactured for this project and extensively equipped with aerodynamic sensors, as well as surface pressure high-frequency microphones flush-mounted in the outer part of the blade which are relevant for studying aeroacoustic emissions. Some noise measurements according to the IEC-64100-11 standard also exist and may become part of the present benchmark once this has been negotiated and agreed with the current owner of these data.

The first objective of this comparison benchmark is to make sure that the noise predictions from the different codes are based on (nearly) identical aerodynamic data. Indeed, aerodynamic noise is by essence driven by aerodynamic quantities. In this respect, this benchmark is actively connected to the IEA Wind TCP Task 29 Phase IV which currently focuses on using the DANAERO database to validate aeroelastic codes for wind turbines. Therefore, the present study also includes the validation of a restricted set of aerodynamic data considered as crucial for accurately evaluating the noise emissions. The validation of the aerodynamic noise predictions is the core objective of the present benchmark. This is dealt with in two steps. Firstly, the surface pressure fluctuations measured with high-frequency microphones on the blades can be used to partly validate noise prediction codes, particularly for trailing edge noise but possibly turbulent inflow noise as well. Secondly, the noise emissions of the whole turbine in different configurations are investigated.

2. General description of the benchmark

2.1. Generalities

The present benchmark is a combination of a series of code validation through simplified test cases and actual measurement data. In the simplified cases, the analysis of the results should reveal some shortcomings of the actual numerical models and their implementation. In particular, some of these test cases will assume axial symmetry of the flow around the rotor axis and this symmetry should be reflected in the computed results, both aerodynamic and acoustic ones. Furthermore, comparisons between results from the various codes should bring some light on the various methods, assuming that high-fidelity models such as CFD can be taken as reference. Concerning the use of actual measurement data, those collected during the DANAERO experiment will be considered.

Briefly, the DANAERO experiment is a series of measurement campaigns conducted in year 2009



Fig. 1 The NM80 wind turbine in Tjæreborg

on a 2.3MW NM80 wind turbine with a hub height of 60 m [5] (see Fig. 1). One of the three blades of the turbine was specifically manufactured for this experiment and equipped with multiple sensors. Aerodynamic sensors (pressure taps, Pitot tubes, microphones) are distributed along the blade span at several given radii (see Fig. 2). The blade is a LM38.8 m attached to the hub at a radius of 1.24 m from the rotor centre. Therefore, the rotor radius at the blade tip is 40.04 m. A met mast located near the turbine was used to monitor atmospheric conditions. The project also included a series of wind tunnel experiments for which 2D reproductions of given blade airfoil sections were measured. These are not considered as part of the present benchmark so far. Note that surface pressure microphones were flush-mounted on the blade near the outer most instrumented radial section. These measurements are quite relevant for the validation of noise emission models (i.e. trailing edge noise, and possibly turbulent inflow noise).

In the present benchmark, we are interested in validating:

- The aerodynamic part for the wind turbine noise codes using pressure tap sensors and Pitot tubes. These validations are a subset of those conducted as part of Task 29 Phase IV Case IV.1 and therefore mainly orientated toward participants to the present benchmark who do not participate to Task 29.
- The estimation of turbulent boundary layer quantities near the trailing edge relevant for trailing edge noise modeling. These quantities were not measured during the measurement campaigns, but validation will be based on cross- checking the results obtained by the various participants (and existing experience on this type of data, e.g. BANC benchmark [2]).

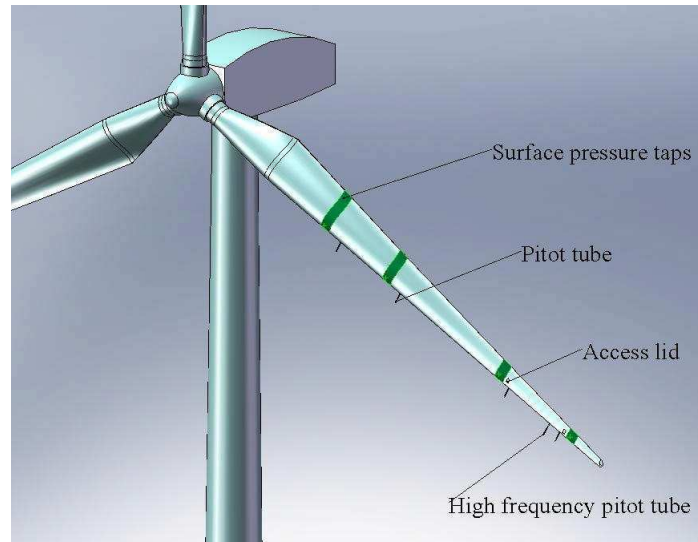


Fig. 2 Equipment on the LM 38.8 m blade

- The estimation of the surface pressure fluctuations (more specifically their spectra) for simulation codes using an approach that do provide such quantity. This validation is mainly relevant for turbulent inflow and trailing edge noise prediction models. The validation can be performed using measurement data from surface pressure microphones on the test blade.
- The prediction of the acoustic noise immission in the far-field (in fact at the distance recommended by the IEC 61400-11 standard). The participants are expected to provide their turbulent inflow and trailing edge noise predictions, but may also include other noise sources (e.g. separation noise if separation is detected, tip noise) if they wish so.

Furthermore, according to the previous description of the benchmark, the benchmark is divided into 3 rounds:

- Round #1 is concerned with the validation of the codes for four idealized cases including symmetrical cases, as well as rigid and flexible rotors. Two parameters are varied in order to quantify their influence on the acoustic results: the rotor rotational speed and wind shear.
- Round #2 is concerned with actual cases from the DANAERO experiment. The specific aim of this round is to compare numerical results with existing measurement data.
- Round #3 is concerned with comparisons of the wind turbine noise codes by calculating noise characteristics as a function of wind speed. Noise was not measured as part of the DANAERO experiment, but noise measurements were conducted as part of the certification procedure for this turbine and may possibly be used in this round for validation. For the time-being, the description of Round #3 is tentative and will be refined at a later stage.

Note that the two first rounds are integrated parts of IEA Wind TCP Tasks 29 & 39, while the third round is more orientated toward participants of Task 39. In this paper, we are only interested in the first round of this benchmark.

2.2. Test cases

As mentioned above, the benchmark is divided into 3 rounds. Each round contains a number of test cases to be simulated. The specific geometrical and aerodynamic inputs for each test case are shortly described in this section for Round #1. The results to be provided are specified in the following section.

For the **Round #1**, there are 4 test cases defined as follows:

Case 1.1

Same as Task 29 Case IV.1.1 and provide comparison results (i.e. aerodynamic and boundary layer quantities, surface pressure near leading and trailing edge, and immission noise) as specified in Section 3 below. The specifications of Case IV.1.1 amounts to an axi-symmetric configuration (no-rotor tilt or yaw, no tower shadow, no wind shear, no inflow turbulence, but the pre-bend is included) and a rigid rotor (i.e. no aeroelastic deformation of the blades).

Case 1.2

Same as Task 29 Case IV.1.2 and provide comparison results as specified in Section 3 below. The specifications of Case IV.1.2 are identical to Case IV.1.1, but for flexible blades. However, if the participant's wind turbine noise code cannot handle flexible blades, this case should be ignored and the participant should carry on with the following cases, assuming a rigid structure in Round #2 (see below).

Case 1.3

Same as Case 1.1, but with a different rotor speed.

Case 1.4

Same as Case 1.1, but with wind shear.

The main other parameters common to all calculations of Round #1 are reported in Table1. Note that the turbulence intensity and length scale specified herein are only meant for the turbulent inflow noise modeling, not the atmospheric wind speed impacting the turbine for the aero-elastic calculations.

2.3. Results to deliver

The results that participants to the benchmark should deliver can be divided into 4 sets.

The first set is concerned with aerodynamic data at the 3 radius locations along the blades. The quantities of interest are mainly relative velocity (with and without induction), angle of attack, aerodynamic forces (incl. lift and drag) and coefficients (C_L and C_D , respectively), as a function of time and/or blade azimuth angle. In addition, pressure coefficients around the blade are investigated.

The second set of data is related to trailing edge noise modeling. The results to deliver are quantities across the boundary layer near the trailing edge, both on pressure and suction sides, such as velocity profiles, turbulent kinetic energy, turbulent length scales, and integral quantities such as boundary layer thickness or displacement thickness.

The third set is concerned with surface pressure spectra near the trailing edge and the leading edge, which are of potential interest for trailing edge and leading edge noise, respectively.

The fourth and last set are the noise immission levels at pre-defined observer locations around the turbine on the ground, as well as one location at hub height directly downwind of the turbine. This

Table 1 Main computational input parameters for Round #1.

Quantity	Value
Tilt	0°
Coning	0°
Tower shadow	None
Air density	1.231 kg/m ³
Temperature	19°C
Wind speed	$V_H = 6.1$ m/s
Wind shear	None
Turbulence intensity	8.96%
Turbulence length scale	39 m
Rotor speed	12.3 rpm
Blade pitch angle	1.5° (>0 nose down)
Yaw error angle	0°
Transition location	$x/C = 0.065$ (Suction side)
Transition location	$x/C = 0.20$ (Pressure side)

last noise immission location is dedicated to check the sanity of the numerical models with respect to the axial symmetry defined in Round #1 (see above).

3. Preliminary results and comparison examples

As none of the participants have sent their results at the time of writing, some of the expected results are shown in this section in order to illustrate the specificities of the different test cases.

3.1. Aerodynamic results

In figure 3, some aerodynamic data on a given blade at the outer most radial position $r = 37$ m are plotted as a function of its azimuth angular position ψ for the 4 considered test cases. The quantities are the effective velocity, the angle of attack, the lift and drag coefficients. As expected, for test cases 1.1, 1.2 and 1.3 (i.e. without shear), the aerodynamic quantities do not vary with the azimuth position. Contrastingly, these quantities are a function of the azimuth for test case 1.4, which includes a wind shear, thereby breaking the symmetry with respect of the rotor axis as discussed earlier. Note that the angle of attack, as well as lift and drag, are highest when the blade points upwards (i.e. for $\psi = 0^\circ$). Test case 1.3 exhibits a higher effective velocity because of the higher rotational speed. Furthermore, it can be noticed that the blade flexibility for test case 1.2 also modifies the aerodynamic properties with a higher angle of attack, at least at the considered radius.

3.2. Noise immission results

As the main goal of this benchmark is to validate wind turbine noise simulation code, a few examples of noise immission results in the vicinity of the turbine are shown here.

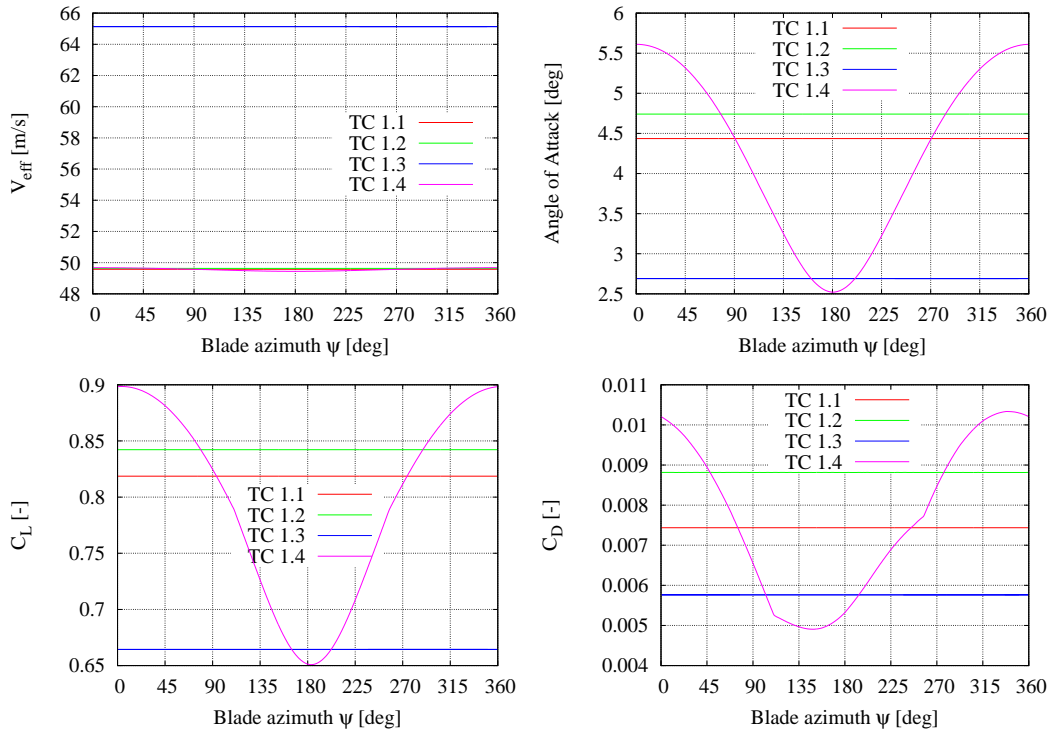


Fig. 3 Aerodynamic quantities as a function of blade azimuth location ($\psi = 0^\circ$ when the blade points up)

The whole turbine noise immissions (i.e. the contributions of the noise emissions are integrated over the whole span of the 3 blades and over the whole frequency range) for the 4 test cases are plotted as a function of the azimuth of blade #1 during one of its revolution in Figs. 4, 5 and 6. In the first two figures, the immission location (denoted as P13) is directly downwind of the rotor at hub height. Therefore, this latter point is located on the rotor axis since the rotor is not tilted. In the third figure, the immission point (denoted as P7) is at the IEC standard position, directly downwind of the turbine on the ground. Furthermore, in these figures the noise levels are displayed by adding up all considered noise sources, i.e. here turbulent inflow noise, trailing edge noise and stall noise, as well as individually in the separate sub-figures.

As expected for the results at P13 in Fig. 4, the symmetry of the flow for test cases 1.1, 1.2 and 1.3 results in constant noise levels. However, for an asymmetrical flow field (i.e with wind shear for test case 1.4), the noise levels exhibit temporal variations, in particular for the trailing edge and stall noise, whereas the turbulent inflow noise appears insensitive to the wind shear. The overall noise is slightly influenced by the shear. In the case of A-weighted noise as displayed in Fig. 5, the stall noise becomes dominant and the temporal variation of noise levels become apparent for the overall noise. It may be surprising that stall noise is dominant in the present configuration. This is investigated below. Before that, it should be noted that the noise immissions at P7 in Fig. 6 illustrate the fact that this position breaks the symmetry of the noise emission as a result of the noise sources directivity.

In order to study the noise emissions in more details, map of the noise sources across the rotor disk are plotted, once again both for all added-up noise sources and individually. These maps represent the elementary contribution to the noise immission levels at given observer locations (i.e.

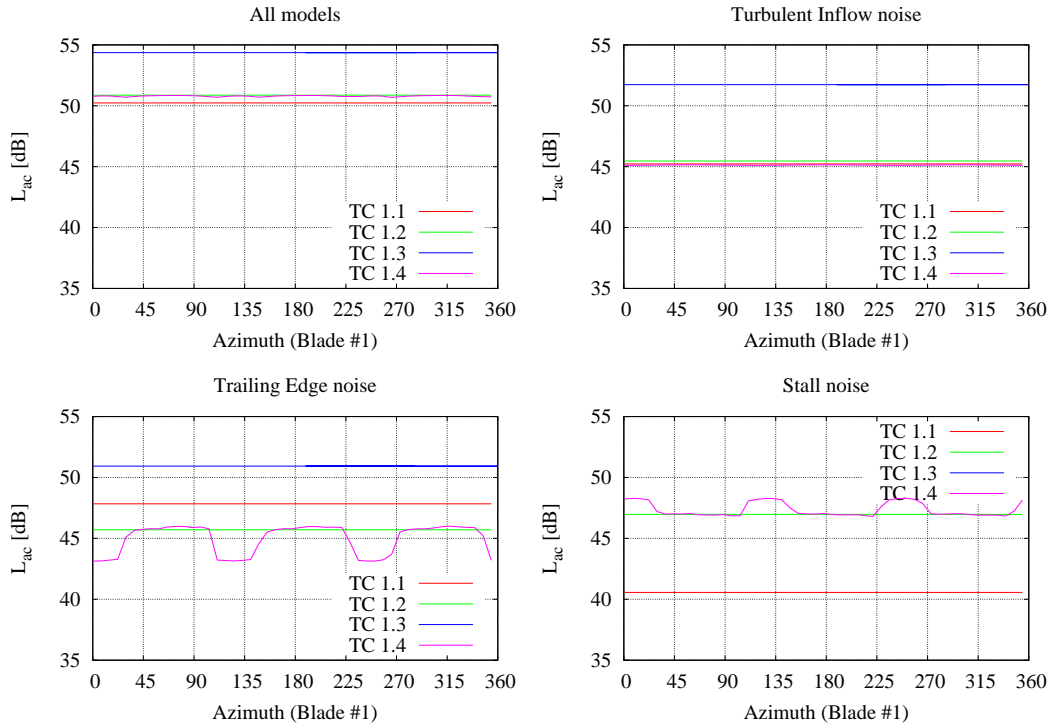


Fig. 4 Noise immission at P13 (downwind of rotor at hub height) as a function of blade #1 azimuth location

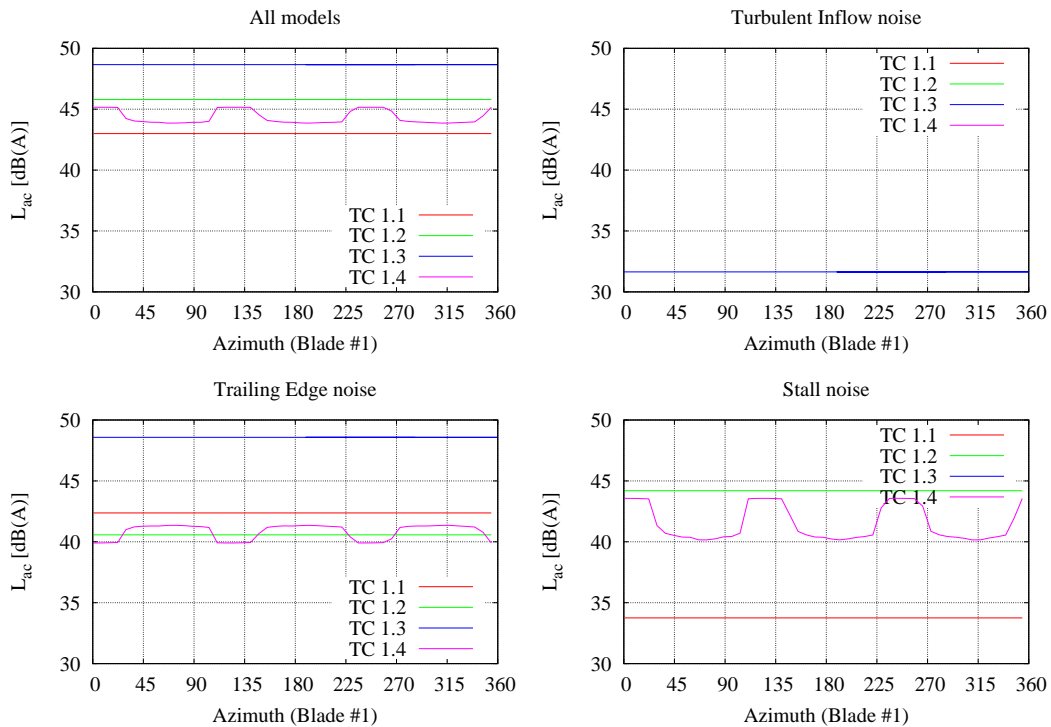


Fig. 5 A-weighted noise immission at P13 (downwind of rotor at hub height) as a function of blade #1 azimuth location

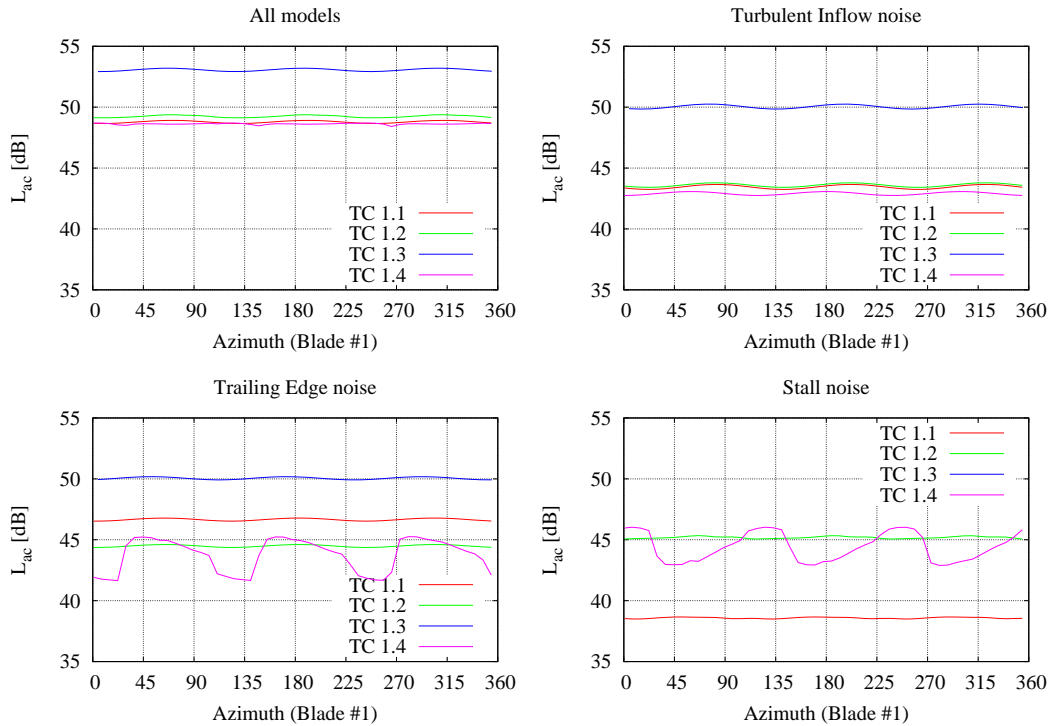


Fig. 6 Noise immission at P7 (downwind of rotor on the ground) as a function of blade#1 azimuth location

P7 or P13 here) from the local noise emissions across the rotor disk. Let us first consider test case 1.1. The map for position P13 is displayed in Fig. 7. The symmetry of the noise emissions is clear. Furthermore, it can be seen that stall noise is concentrated in the inner region of the rotor disk/blade where thick airfoil sections can be found, more easily triggering the occurrence of stall. The same map but for position P7 is displayed in Fig. 8. Once again, the asymmetry from the noise directivity patterns becomes apparent and it can be seen that higher noise levels are observed on the lower right part of the rotor disk, both for turbulent inflow and trailing edge noise. This effect is possibly a combination of directivity and the fact that the lower part of the rotor disk is closer to the observer at P7.

Finally, the noise map for test case 1.4 (with wind shear) for an observer at position P13 is displayed in Fig. 9. It can be seen that stall noise is produced on a large upper part of the rotor disk. Indeed, it is where the wind speed is higher due to the wind shear and angles of attack are also larger (see Section 3.1). However, it was observed in the previous section the angles of attack remain relatively low and it is quite surprising that stall is so widely spread. This indicates a potential problem in the simulation code which has to be investigated (or alternatively a misinterpretation of the results). As a matter of fact, one of the primary goal of the present benchmark is to detect such inconsistencies in the results and try to improve the prediction tools accordingly.

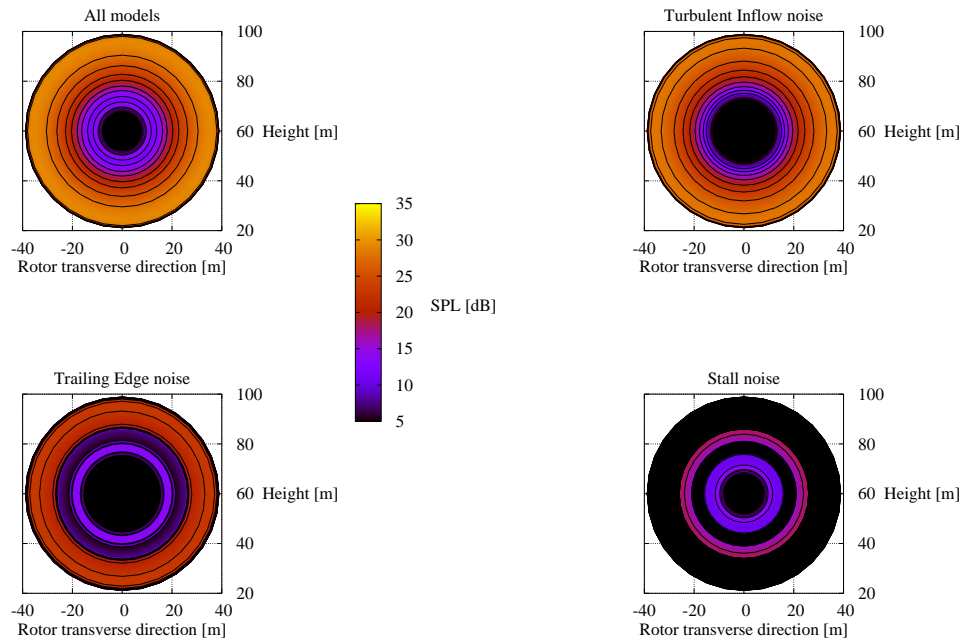


Fig. 7 Noise immission map at P13 (downwind of rotor at hub height) as seen from upwind the turbine - Test case 1.1.

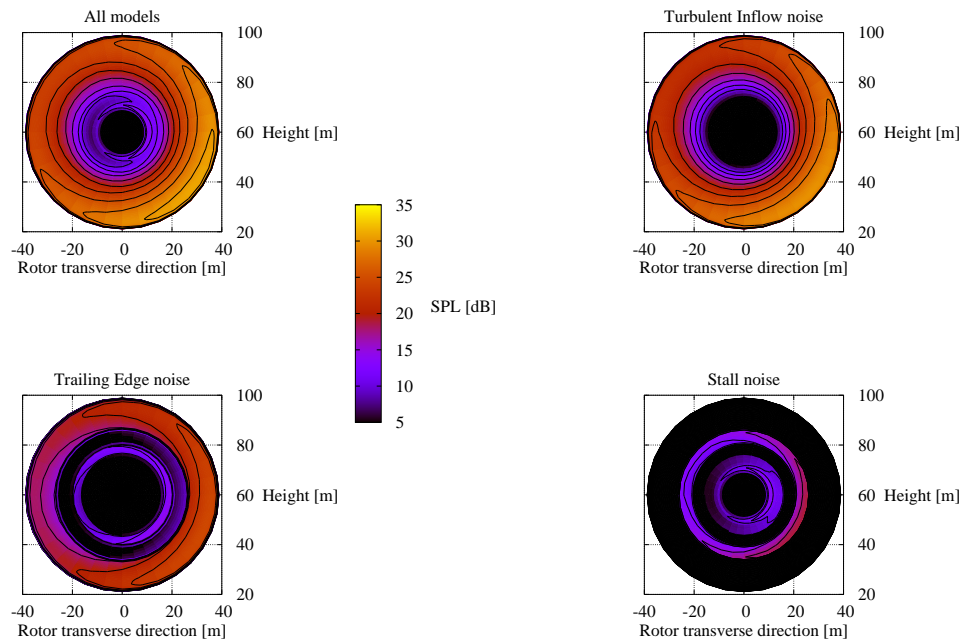


Fig. 8 Noise immission map at P7 (downwind of rotor on the ground) as seen from upwind the turbine - Test case 1.1.

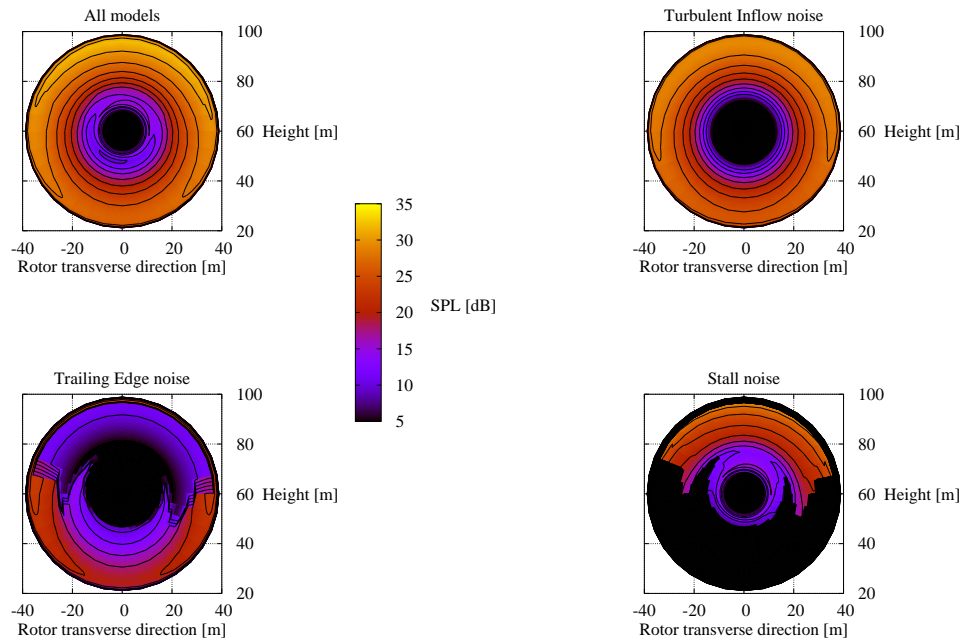


Fig. 9 Noise immission map at P13 (downwind of rotor on the ground) as seen from upwind the turbine - Test case 1.4.

4. Conclusion

A benchmark for wind turbine noise simulation codes comparison and validation is proposed. The main details of the numerical inputs to the various test cases have been presented (at least for the first round of this benchmark).

At the time of writing, none of the participants have had time to perform the required computations and send their results. However, it is expected that a number of participants will have conducted these before the start of the conference, and that comparisons and analysis of the results can be presented then.

A tentative timeline for the continuation of this benchmark follows. As mentioned above, it is expected that the results of the first round can be analyzed at the WTN 2019 conference, as well as during the next IEA Wind TCP Task 39 meeting which is planned as a side-event to the conference. Round #2 should be conducted during the second semester of year 2019, and Round #3 probably during the first semester of year 2020. However, conclusions from the initial analyses may alter this timeline. In particular, it may be necessary to come back on specific issues of the test cases if difficulties in understanding the results and their comparisons do arise.

Acknowledgments

This work was partly supported by the EUDP-2016 project Jr.nr. 64016-0056 funded by the Danish Energy Agency (Energistyrelsen). In addition, the present benchmark is conducted as a sub-task of the IEA Wind TCP research Task 39 (Quiet Wind Turbine Technology), as well as a part of IEA Wind

References

- [1] Arcondoulis, E. J. G., Doolan, C. J., Zander, A. C., and Brooks, L. A. (2010). A Review of Trailing Edge Noise Generated by Airfoils at Low to Moderate Reynolds Number. *Acoustics Australia*, 38(3):135–139.
- [2] Herr, M., Ewert, R., Rautmann, C., Kamruzzaman, M., Bekiropoulos, D., Iob, A., Arina, R., Batten, P., Chakravarthy, S., and Bertagnolio, F. (2015). Broadband Trailing-Edge Noise Predictions - Overview of BANC-III Results. In 21th *AIAA/CEAS Aeroacoustics Conf. (Proc.)*, AIAA Paper 2015-2847, Dallas (TX).
- [3] Hutcheson, F. V. and Brooks, T. F. (2006). Effects of Angle of Attack and Velocity on Trailing Edge Noise Determined Using Microphone Array Measurements. *International Journal of Aeroacoustics*, 5(1):39–66.
- [4] IEC (2012). International Standard, Wind Turbines - Part 11: Acoustic Noise Measurement Techniques. IEC 61400-11, International Electrotechnical Commission, Geneva (CH). ISBN 978-2-83220-463-4.
- [5] Madsen, H. A., Bak, C., Paulsen, U. S., Gaunaa, M., Fuglsang, P., Romblad, J., Olesen, N. A., Enevoldsen, P., Laursen, J., and Jensen, L. (2010a). The DAN-AERO MW Experiments. In 48th *AIAA Aerospace Sciences Meeting Including The New Horizons Forum and Aerospace Exposition (Proceedings)*, AIAA Paper 2010-645, Orlando (FL).
- [6] Madsen, H. A., Bak, C., Paulsen, U. S., Gaunaa, M., Fuglsang, P., Romblad, J., Olesen, N. A., Enevoldsen, P., Laursen, J., and Jensen, L. (2010b). The DAN-AERO MW Experiments - Final report. Tech. Rep. Risø-R-1726(EN), Risø-DTU, Roskilde, Denmark.